AJAE

Open Access

Vol. 14, No. 4, pp. 413-421, December 2020
doi: https://doi.org/10.5572/ajae.2020.14.4.413
ISSN (Online) 2287-1160, ISSN (Print) 1976-6912

Technical Information

Application of Chemical Ionization Mass Spectrometry in Airborne SO_2 Observation on Hanseo Beechcraft 1900 D

Jinsoo Park, Jinsoo Choi, Kwangjoo Moon, Danbi Kim, Hyun-Jae Kim, Joonyoung Ahn, Sangwook Lee, Beom-Keun Seo[1)], Jongho Kim[1)], Soobog Park[2)], Saewung Kim[3),*]

Climate and Air Quality Research Department, Air Quality Research Division, National Institute of Environmental Research, Incheon, Republic of Korea
[1)]Institute of Environmental Research, Hanseo University, Seosan, Republic of Korea
[2)]Department of Flight Operations, Hanseo University, Seosan, Republic of Korea
[3)]Department of Earth System Science, School of Physical Sciences, University of California, Irvine, Irvine, California, U.S.A.

***Corresponding author.**
Tel: +1-949-824-4531
E-mail: saewung.kim@uci.edu

Received: 27 June 2020
Revised: 25 August 2020
Accepted: 17 September 2020

ABSTRACT As the observational constraints of SO_2 become a limiting factor for emission inventory and regional and global transport model validations, we present an airborne SO_2 observational suite integrated on Beechcraft 1900D (B1900D) operated by Hanseo University. A chemical ionization mass spectrometry (CIMS) technique using SF_6^- ion chemistry is used to take advantage of fast response (<1 Hz) and the low limit of detection (30 ppt). In this study, we describe the performance of the CIMS system on B1900D along with descriptions on the modified airborne platform. Furthermore, exemplary observational results around point sources such as a steel production facility and a petrochemical industrial facility in the Taeahn Peninsula in South Korea. In addition, an observational result over the Yellow Sea is presented to demonstrate the ability of the instrumentation to capture pollution transport from the continent. Overall, the performance of the airborne CIMS system for SO_2 is well demonstrated for future air quality studies.

KEY WORDS SO_2, sulfur dioxide, Air pollution, CIMS, Point source, Airborne

1. INTRODUCTION

Sulfur is not necessarily a dominant element in the composition of the Earth. In this context, it is rather surprising that sulfur compounds, mostly sulfate (SO_4^{2-}) composed the substantial fraction fine aerosols (e.g. $PM_{2.5}$). Most of the sulfur in the condensed phase in the troposphere is originated from gas phase compounds through atmospheric oxidation (Davis *et al.*, 1998). Before the human impacts to the atmospheric composition were not significant, mostly natural activities maintained the sulfur levels in the atmosphere such as SO_2 from volcanos and dimethylsulfide (CH_3SCH_3) from phytoplanktons (Davis *et al.*, 1999). Once emitted, oxidation processes both homogeneous and heterogeneous pathways eventually chemically convert to the most oxidized form of sulfur (S (VI)) such as SO_4^{2-} and H_2SO_4 (g), which have substantially lower vapor pressure to be partitioned to the condensed phase (Jacob, 1999).

Since the industrial revolution, sulfur emission from anthropogenic activities

associated with coal burning has been explosively increasing. The emissions from anthropogenic activities now are mostly composed by electricity generation, industrial, and mobile sources mostly coal burning activities and residual sulfur emission from under processed diesel fuel (Ohara *et al.*, 2007).

In recent years, Europe and North America have shown substantial decrease in anthropogenic SO_2 emissions mainly due to changes in the electricity generation portfolio. In contrast, SO_2 emissions in Asia had been rapidly growing since 1990 mostly driven by the economic development in China (Ohara *et al.*, 2007). Recent emission inventory assessments and satellite observations clearly shows the decreasing trend from mid-2000 over China. South Korea, the more advanced stage of the energy use and the economic development, the decreasing trend of SO_2 emission has been observed in the earlier time frame since mid 80s. Currently, the SO_2 mixing ratio of 150 ppb or higher in one hour average is considered as the out of compliance in the South Korean environmental regulation. Although the out of compliance level of SO_2 never observes in the ambient air except the fresh plumes of combustion exhausts in the industrial facility, it is still a great deal of scientific interests to precisely constrain SO_2 emissions as it propagates into ambient aerosol loading estimates that have tremendous implications to regional to global air quality and climate. Especially, as the local air quality policy requires the quantitative assessment on relative contributions from local vs trans-boundary pollution, precise emission monitoring becomes more important.

It has been a conventional method that inverse modeling is a main tool to calculate top-down emission inventory. Recently, satellite SO_2 products (a column density) has started to be implemented in the inverse model framework. Lee *et al.* (2011) reported a substantial discrepancy between bottom-up and top-down SO_2 emission estimates in China although a consistency between the two was found in the United States. The consistent problem in the Asian region has been reported by Aas *et al.* (2019) and Qu *et al.* (2019). This finding most likely reflects the rapid changes in emissions in the Asian region.

To better characterize the rapidly changing SO_2 emission, it is important to observationally constrain large emission sources with the high temporal resolution to monitor changes in different activities for the facilities. Especially, considering the poor spatial resolution of satellite observation, it is imperative to monitor the SO_2 emission using in situ techniques. Airborne platforms have a great advantage to monitor the spatial distribution of trace atmospheric constituents in a fast time resolution, which make it ideal for the emission estimates with proper meteorological measurements. In addition, the airborne observation has been using a powerful tool to investigate transboundary air pollution problems (e.g. NIER and NASA, 2017). This motivates us to present this study of characterizing a recently developed airborne platform Beechcraft 1900 D (Hanseo B1900D, HL5238) owned and operated by Hanseo University in South Korea. In this study, we describe improvements made on Hanseo B1900D to adapt research grade atmospheric chemistry instrumentation and proper sample introduction. In addition, an introduction to the analytical characteristics of SO_2 and meteorological sensors on-board is presented to discuss how the combination of the datasets can directly constrain SO_2 emissions for large point sources and capture elevated SO_2 over the Yellow Sea.

2. METHODS

2.1 Hanseo B1900D

In February 2019, Hanseo B1900D was modified for the atmospheric chemistry research. The underlying considerations for the modifications are described as next;

1) The mission power for the scientific payload has separate generator circuits from the aviation related power supplies so that any potential power interruption would not interfere the aviation safety.
2) After mission power is generated, it goes through six independent inverters (DC 28 V to AC 230 V 50 Hz) to provide power to eight independent power stations, distributed to the cabin. The cabin layout and distribution of the power stations are shown in Fig. 1. The design prevents any power interruption caused by an incident happening to one power station.
3) There are only one prefixed instrument rack containing inverters, a data logger for a meteorological sensor, and other housekeeping accessories. All other scientific payload can be integrated in an instrument

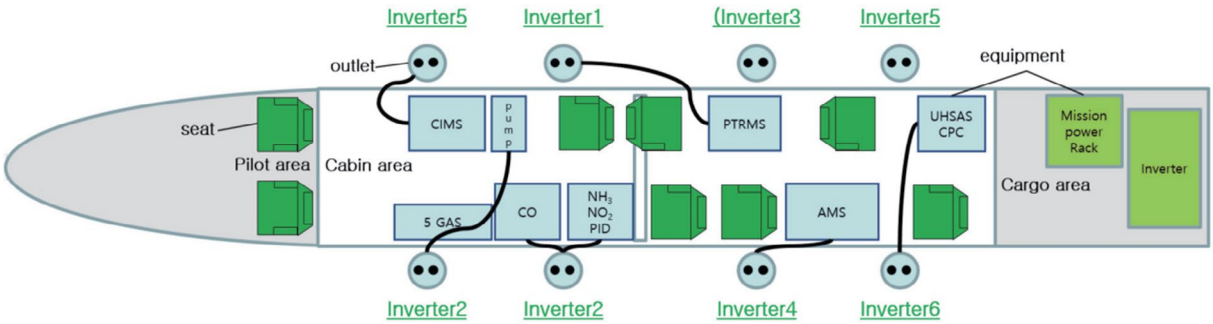

Fig. 1. The cabin layout of B1900D and distribution of the power stations.

rack to be fastened using the seat rails to maximize the flexibility of the platform.

4) Four gas phase inlet systems are installed two window plates located in the starboard and the port side windows in the very front of the plane to prevent any interference from the engine exhaust. Two aerosol inlet systems (DMT - part number AAA-0151for a heated inlet and AAA-0093 for unheated inlet) are mounted top of the fuselage. They are also located in the front part of the fuselage to prevent engine exhaust interferences.
5) ARIM200 Digital Air Data Probe (Aventech Research Inc. Ontario, Canada) is installed on the forward port side of the fuselage. The potential interference from the turbulent interaction between ambient air and fuselage was thoroughly considered from the planning stage and implemented in the modifications.

The overall modification goals are the outcome of discussion in the South Korean scientific community. The goals were implemented by Global Aviation Technology in Wichita, Kansas U.S.A. to be satisfied with the aircraft engineering capacity and the Federal Aviation Administration regulations. The FAA certified engineering plan was implemented by Air Asia, Tainan City, Taiwan.

2.2 The AIMMS-30 System

AIMMS-30 (Aventech Research Inc. Barrie ON Canada) on Hanseo B-1900D is consisted by an ARIM200 Air Data Probe system, a VECTRAX 10 Inertial Altitude Unit system, and a MetTrack display and general interface system. ARIM200 a digital electronic air data sensing system is capable of measuring atmospheric pressure, altitude, air speed, angle-of-attack, temperature, relative humidity, and the speed and the direction of the aircraft-relative wind vector.

ARIM200 contains the 5-hole probe head for the resolution of airflow angles and pitot pressure. The signals from sensors transfer through a Controller Area Network (CAN) bus to the VECTRAX system. It also receives two global positioning system (GPS) signals from antennas mounted on fuselage. With the data stream, it processes data and save it as a binary file. Calibration maneuvering based upon Lenschow (1986) with the consideration to retrieve accurate 3D wind dataset on a fast-moving platform such as aircraft.

The system is compact enough to be integrated a mid-size aircraft such as Hanseo B-1900D. The capability to accurately quantify meteorological variables is essential to assess turbulent and advective fluxes discussed in the result section.

2.3 Chemical Ionization Mass Spectrometer

A chemical ionization mass spectrometer (THS Instruments LLC, Atlanta GA USA) was used for SO_2 quantification on Hanseo B1900D. It has been used the main SO_2 quantification tool on NASA DC-8 Airborne Laboratory since the INtercontinental Transport EXperiment (INTEX) in 2004 (Kim *et al.*, 2007). A detailed analytical system is thoroughly discussed Kim *et al.* (2007). It is utilized SF_6^- as a reagent ion. SF_6^- ion is generated from 0.1% of SF_6 mixture (5–10 standard cc minute^{-1}) balanced with N_2 using N_2 as a carrier gas (2 standard liter minute^{-1}). The ionization of SF_6 is triggered by α particles from Po-210.

Ionization of SO_2 by the reagent ion is facilitated in a flow tube - a 5-inch long QF-40 nipple maintained ~10 torr of pressure. 1slpm of ambient air is introduced to the flow tube to selectively ionize ambient SO_2 as;

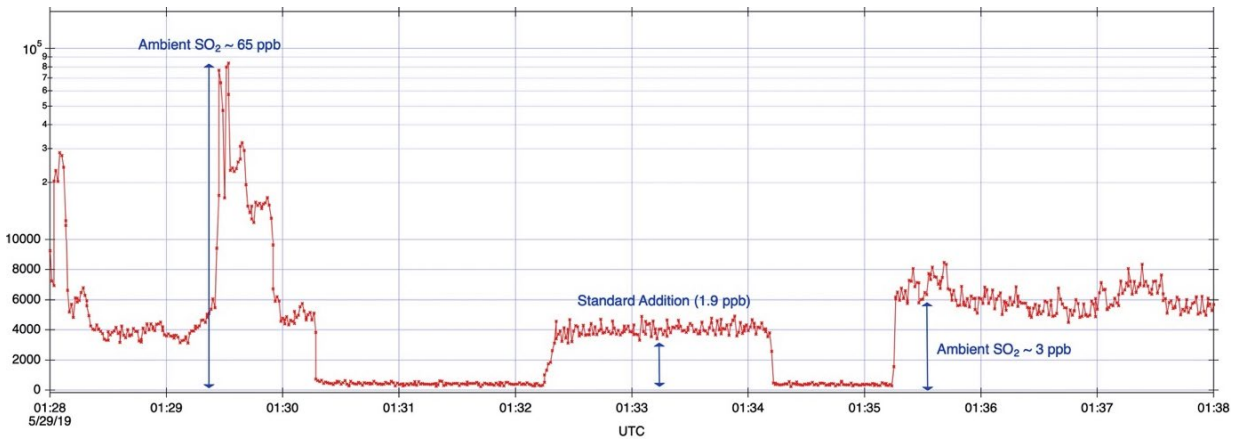

Fig. 2. A temporal variation of $SO_2F_2^-$ signal during an airborne observation near a point source.

$$SO_2 + SF_6^- \rightarrow SO_2F_2^- + SF_4$$

$$SO_2 + SF_6^- \rightarrow SO_2F_2^- + SF_5$$

We monitor both masses along with the isotopic mass of $^{34}SO_2F_2^-$ as the trace can be useful to correctly quantify SO_2 in the power plant plume with extremely high SO_2 (100 ppb or higher) when the count statistics of the detector gets into the non-linear range.

Once the ion generated, the ion beam passes through a collision dissociation chamber where an octopole system is optimized to break up ion clusters. Ion beam then introduced the main chamber with an octupole system for ion focusing and the quadrupole chamber for the mass filtration finally to the channeltron detector. Overall system is monitored and controlled one laptop with a custom-made software on the LINUX platform.

3. RESULTS AND DISCUSSION

3.1 The Performance of CIMS SO_2 Quantification System

As discussed, the in-flight calibration functionality both background and sensitivity checks are equipped. The time series of raw signals during the flight is shown in Fig. 2. The calibration can be programed so that the process is conducted in the predetermined period. The mass spectrometer is configured to hop a list of masses in around 1 second period. Each mass is set to be monitored 100 ms (millisecond). Fig. 2 clearly illustrates the advantage of the high temporal frequency observations. The nominal true air speed for the research flight is maintained ~85 m s^{-1}. Therefore, it covers ~500 m in one minute, which one can easily miss nearfield plumes from industrial facilities with a low time resolution instrument. On the other hand, Fig. 2 clearly demonstrates that we can capture the plumes.

Table 1. Bottom-up SO_2 emission estimates published in CAPSS by Ministry of Environment in South Korea.

CAPSS 2015	SO_2 (kg yr^{-1})
Dangjin Power Plant	7,016,148
Boryung Power Plant	13,253,039
Taehan Power Plant	13,085,660
Hyundai Steel Manufacturing Facility	11,702,268
Daesan Petrochemical Facility	13,855,763

In such a high frequency, it is important to have a low limit of detection and high sensitivity a strong analytical advantage of the CIMS system (Huey, 2007). During the research flight, the limit of detection is consistently estimated 30 ppt for the one second average (1σ) and 4 ppt for one-minute average (1σ). The system demonstrates the nominal sensitivity of 3 Hz ppt^{-1}. In addition, the system demonstrates a wide linear range from the detection limit to the high SO_2 levels (up to 400 ppb), which is critical for accurate quantifications for near field pollution plume in the background conditions.

3.2 SO_2 distributions in the South Korean West Coast

The West Coast in South Korea has a complicated SO_2 emission sources as there are a wide range of emis-

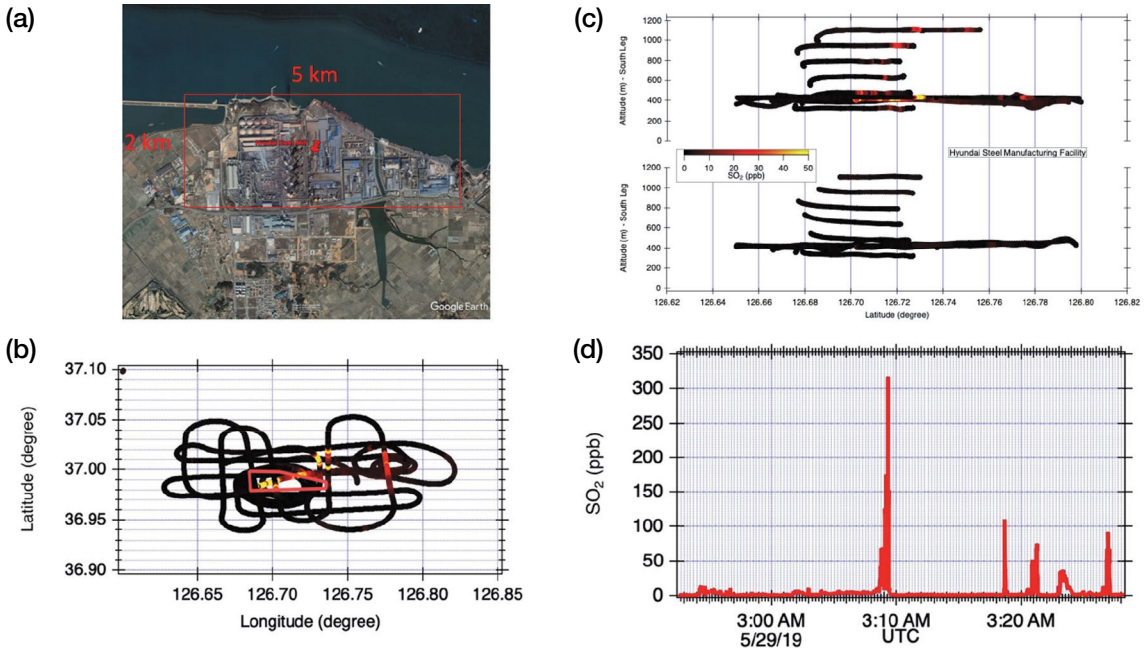

Fig. 3. A SO_2 observational dataset over Hyundai Steel Manufacturing Facility (a). (b) Horizontal distribution of SO_2 with the SO_2 mixing ratio color coding. The red outline shows the border of the facility. (c) A SO_2 curtain plot to illustrate the vertical distribution. The y-axis represents altitude and the x-axis is longitude. The upper panel shows the north wall and the lower one shows the south wall. The cut-off latitude of 36.98°N was used to generate the curtain plot. (d) A time series of SO_2 over the observational track. The highest concentration (~300 ppb) was observed inside of the facility.

sion sources and it is susceptible to an influence of continental outflow. The estimated SO_2 emissions in Clean Air Policy Support System (CAPSS) is summarized in Table 1. The region is consisted the largest SO_2 emission in South Korea. Here, we present representative airborne SO_2 observational results.

3.2.1 Hyundai Steel Manufacturing Facility

An example of SO_2 observations for Hyundai Steel Manufacturing Facility is shown in Fig. 3. As shown in the Google Earth image, there are multiple chimneys in the facility. The highest concentration was observed during the overpass of the facility (300 ppb). Due to the Southwestery wind, it is clear that the SO_2 plume is spreading towards Northeast. Vertical curtain plots (Fig. 3c) clearly show that SO_2 plume is spreading in a well-defined fashion, which illustrates that the applied maneuvering pattern is successfully captured SO_2 emission from the facility. In contrast, there is no significant elevation of SO_2 in the upwind cross-section. Therefore, the observational dataset can be used to calculate the instantaneous emission rates. The observed SO_2 distributions around the coal power plants - Danjing, Taeahn, and Boryung show also the similar SO_2 distribution - a distinguished plume pattern.

This observation vouches the application of a Gaussian plume model. It is a model framework established in 1940 (Weil and Brower, 1984). It describes the concentration distribution of pollutants emitted from an industrial stack by a descriptive mathematical equation (Eq. 1).

$$C(x,y,z) = \frac{Q}{2\pi u \sigma_y \sigma_z}\left\{\exp\left(\frac{-(z-h)^2}{2\sigma_z^2}\right) + \exp\left(\frac{-(z+h)^2}{2\sigma_z^2}\right)\right\}\left\{\exp\left(\frac{-(y)^2}{2\sigma_y^2}\right)\right\} \quad \text{(Eq. 1)}$$

where,

C: Pollutant Concentration

Q: Emission Rate from a stack

u: horizontal wind speed

σ_z: vertical wind distribution - a function of stability and a horizontal distance (x)

σ_y: cross wind distribution - a function of stability and a horizontal distance (x)

The spatial distribution of emission can be described

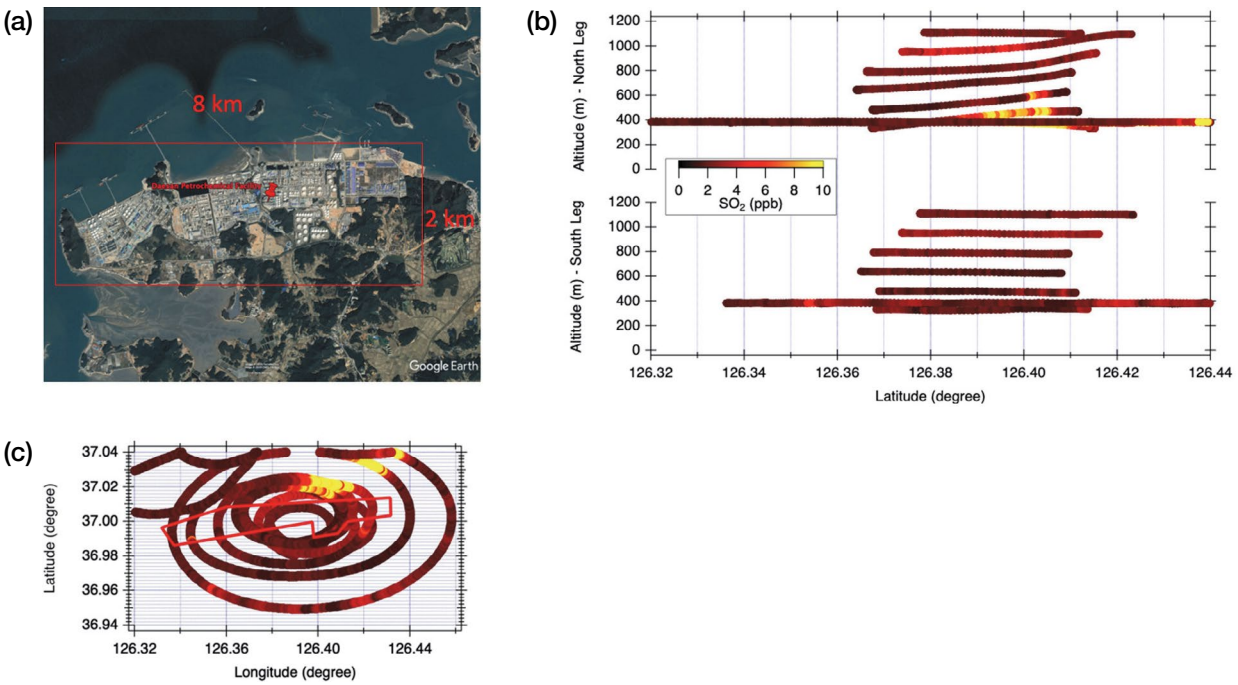

Fig. 4. (a) A satellite view of the Daesan Petrochemical Facility. (b) The observed horizontal SO_2 distribution. The border of the facility is shown with a red line. (c) A curtain plot color coded with SO_2 concentration. The north and the the south walls are presented in the upper and the lower panels, respectively. The latitude line of 39.9°N was used to separate the North and South.

simply by wind speed, wind direction, and atmospheric stability classes that can be evaluated by the vertical distribution of air temperature. As all these parameters are monitored by AIMMS-30, we can apply the Gaussian plume model equation to calculate instantaneous emission rates (kg hour^{-1}). We choose one observed plume that has the highest concentration of SO_2, which is also consistent with wind direction. We then assume the spot is the center of the Gaussian plume to calculate the instantaneous emission rate using Eq. 1. Certainly, this approach has limitation as it ignores other diverted plumes that we can clearly observe in the spatial distributions of SO_2, illustrated in Fig. 3. In addition, as the emissions from multiple stacks rather than one stack that is an assumption of the proposed calculation, this will also contribute to underestimate total SO_2 emission from the given point source. For example, if the identical amount of SO_2 is emitted in five different chimneys separated 60 m each, the concentration of SO_2 in the center of the plume, observed 2 km away from the emission is 60% lower than the assessed highest concentration calculated under the assumption, which all the SO_2 emission from one stack. In this context, the calculated instantaneous emission rate in this presented method should be considered a low-end estimate. To evaluate bottom-up emission estimates based upon the instantaneous emission estimates, it requires frequent observations over the extended time frame to accumulate a statistically relevant dataset. By applying the plume model with a neutral stability, we calculated instantaneous SO_2 emission rate of 3483 kg hour^{-1}. We have utilized the wind dataset from the AIMMS-30 system to calculate the flux. Although this is substantially higher than the hourly emission rate, deduced from the annual emission rate (~three times), presented in Table 1, More frequent observation is necessary to be more statistically relevant.

3.2.2 Daesan Petrochemical Facility

As shown in Table 1, Daesan Petrochemical Facility is also emitted a substantial amount of SO_2. Unlike the previously described powerplant and steel manufacturing facility examples, SO_2 emission in the facility is spread around a large facility consisted by a number of different factories with different processing functions as shown in Fig. 4.

The observed SO_2 around the Daesan Petrochemical Facility is also consistent with the distributed nature of

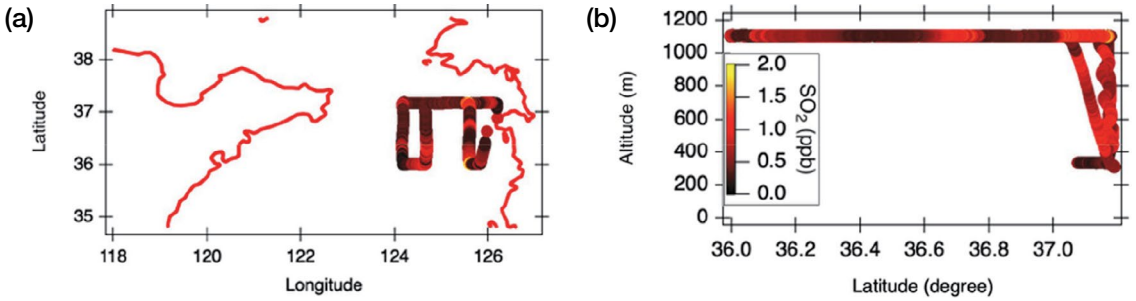

Fig. 5. The horizontal (a) and the vertical distributions (b) of SO_2 quantified from the flight conducted in June 2nd 2019.

SO_2 emission in this facility. In other words, once the plume model is applied in this case, the outcome will only capture the major plume but not more spread around elevated SO_2. Therefore, it may not be relevant to apply the Gaussian plume model. Gordon *et al.* (2015) presented a model framework to account emission of aerial sources. Emission from point or aerial sources can be described following elements

$$E_C = E_{CH} + E_{CHT} + E_{CV} + E_{CVT} + E_{CVC} - E_{CM} - E_{CX} \quad \text{(Eq. 2)}$$

where,

E_C: the total emission rate integrated over all activities within the source

E_{CH}: the horizontal advective flux through the box walls

E_{CHT}: the horizontal turbulent flux through the box walls

E_{CV}: the advective flux through the top box

E_{CVT}: is the turbulent flux through the box top

E_{CVD}: is the deposition to the surface

E_{CM}: the increase in mass within the volume due to a change in air density

E_{CX}: the increase in the mass due to chemical changes of the compound within the box volume

In general, the last three terms are not considered in emission estimates because they are insignificant. As most of the emission can be accounted E_{CH}, Gordon *et al.* (2015) has developed a model framework to characterize the horizontal advection called the top-down emission rate retrieval algorithm (TERRA). To apply TERRA, it requires a curtain plot pattern sampling, which we demonstrated to observe the vertical distributions of SO_2 around the studied industrial facilities. Then with the observed meteorological and chemical parameters, the algorithm calculated the horizontal advective flux using the following equation.

$$E_{CH} = M_R \iint \chi c \rho_{air} U \, dsdz \quad \text{(Eq. 3)}$$

where,

MR: the ratio of the compound molar mass to the molar mass of air

χc: the average screen mixing ration around the box wall

ρ_{air}: the density of air

U: the horizontal wind speed

A code for the calculation is written in Igor (Wavemetrics Inc.). Currently, we are applying the code to calculate the advective flux. The SO_2 flux calculation result using the TERRA model for the Hyundai Steel Mill case, presented in Fig. 3 is 3807 kg hour^{-1}, which is a similar value calculated using the TERRA model framework. The SO_2 flux from the Daesan Petrochemical Facility is estimated as 1306 kg hour^{-1} also by the TERRA model. This instantaneous emission rate is comparable with the deduced emission rate from the annual emission rate. We have utilized the wind dataset from the AIMMS-30 system to calculate the flux.

3.3 SO_2 distributions over the Yellow Sea

As sulfate is a dominant component in fine particles observed in Korea and most of the East Asia, it is important to characterize the sulfur sources. SO_2 is the primary precursor for sulfate. Other than the local industrial sources, it has been a particular research interest to characterize transported SO_2 particularly from China. Obviously, utilizing airborne platforms to capture transported pollution plume is the best option to constrain the transport pathways and amounts. During the KORUS-AQ campaign, most of SO_2 over the Korean Peninsula was attributed from the local contributions. However, a caution should be exercised in the fact that this is the conclusion based upon the observations

while the continental outflows are not active according to the Rapid Scientific Synthesis Report (NIER and NASA, 2017).

We have conducted several research flights to try capturing pollution outflows from China and present an exemplary flight in Fig. 5. The horizontal and the vertical distributions of SO_2 illustrates a clear SO_2 gradient in the range of the lower limit of detection (20 ppt) to 2 ppb. Although, it requires an integrated approach including detailed observational data analysis and model comparisons to attribute the SO_2 sources for the observed SO_2 plumes, the observational results.

4. SUMMARY

We demonstrated the observational capability of SO_2 on Hanseo Beechcraft 1900D modified for airborne atmospheric composition monitoring along with micrometeorological parameters. The fast time response of the CIMS application allows us to sample narrow plumes from point sources. We demonstrated that the observational dataset can constrain instantaneous emission rates of SO_2 from point sources such as coal power plants and steel manufacturing facility along with the micrometeorological dataset. The high sensitivity and the low limit of detection of CIMS in the SO_2 quantification allow us to identify the enhancements of SO_2 over the marine boundary layer in the Yellow Sea that could be originated from pollution outflows from China. As we assess the performance of the analytical technique is suitable for airborne observations for scientific purposes that certainly can provide quantitative diagnostic basis for policy decisions to improve air quality.

This in situ observational capability is expected to provide an essential dataset to validate remote sensing datasets (Chong *et al.*, 2020) and chemical transport model results through coordinating efforts.

ACKNOWLEDGEMENT

This work was supported by National Institute of Environmental Research (NIER-RP0219-152) and the National Strategic Project - Fine Particle of the National Research Foundation of Korea (KRF) funded by the Ministry of Science and ICT (MSIT), the Ministry of Environment (ME), and the Ministry of Health and Welfare (MOHW) (20173D8A1090662).

REFERENCES

Aas, W., Mortier, A., Bowersox, V., Cherian, R., Faluvegi, G., Fagerli, H., Hand, J.L., Kilmont, Z., Gally-Lacaus, C., Lehmann, C.M.B., Myhre, C.L., Myhre, G., Olivie, D., Sato, K., Quaas, J., Rao, P.S.P., Schulz, M., Shindell, D., Skeie, R.B., Stein, A., Takemura, T., Tsyro, S., Vet, R., Xu, X. (2019) Global and regional trends of atmospheric sulfur. Scientific Report, https://doi.org/10.1038/s41598-018-37304-0

Chong, H., Lee, S., Kim, J., Jeong, U., Li, C., Krotkov, N.A., Nowlan, C.R., Al-Saadi, J.A., Janz, S.J., Kowalewski, M.G., Ahn, M.H., Kang, M., Joiner, J., Haffner, D.P., Hu, L., Castellanos, P., Huey, L.G., Choi, M., Song, C.H., Han, K.M., Koo, J.H. (2020) High-resolution mapping of SO_2 using airborne observations from the GeoTASO instrument during the KORUS-AQ field study: PCA-based vertical column retrievals. Remote Sensing of Environment, 241, ARTN 111725, https://doi.org/10.1016/j.rse.2020.111725

Davis, D., Chen, G., Kasibhatla, P., Jefferson, A., Tanner, D., Eisele, F., Lenschow, D., Neff, W., Berresheim, H. (1998) DMS oxidation in the Antarctic marine boundary layer: Comparison of model simulations and field observations of DMS, DMSO, $DMSO_2$, H_2SO_4 (g), MSA (g), and MSA (p). Journal of Geophysical Research-Atmospheres, 103, 1657–1678, https://doi.org/10.1029/97jd03452

Davis, D., Chen, G., Bandy, A., Thornton, D., Eisele, F., Mauldin, L., Tanner, D., Lenschow, D., Fuelberg, H., Huebert, B., Heath, J., Clarke, A., Blake, D. (1999) Dimethyl sulfide oxidation in the equatorial Pacific: Comparison of model simulations with field observations for DMS, SO_2, H_2SO_4 (g), MSA (g), MS, and NSS. Journal of Geophysical Research-Atmospheres, 104, 5765–5784, https://doi.org/10.1029/1998jd100002

Gordon, M., Li, S.M., Staebler, R., Darlington, A., Hayden, K., O'Brien, J., Wolde, M. (2015) Determining air pollutant emission rates based on mass balance using airborne measurement data over the Alberta oil sands operations. Atmospheric Measurement Techniques, 8, 3745–3765. https://doi.org/10.5194/amt-8-3745-2015

Huey, L.G. (2007) Measurement of trace atmospheric species by chemical ionization mass spectrometry: Speciation of reactive nitrogen and future directions. Mass Spectrom Rev, 26, 166–184.

Jacob, D. (1999) Introduction to Atmospheric Chemistry, Princeton University Press, 265 pp.

Kim, S., Huey, L.G., Stickel, R.E., Tanner, D.J., Crawford, J.H., Olson, J.R., Chen, G., Brune, W.H., Ren, X., Lesher, R., Wooldridge, P.J., Bertram, T.H., Perring, A., Cohen, R.C., Lefer, B.L., Shetter, R.E., Avery, M., Diskin, G., Sokolik, I. (2007) Measurement of HO_2NO_2 in the free troposphere during the intercontinental chemical transport experiment - North America 2004. Journal of Geophysical Research-Atmospheres, 112, D12s01, https://doi.org/10.1029/2006jd007676

Lee, C., Martin, R.V., van Donkelaar, A., Lee, H., Dickerson,

R.R., Hains, J.C., Krotkov, N., Richter, A., Vinnikov, K., Schwab, J.J. (2011) SO_2 emissions and lifetimes: Estimates from inverse modeling using in situ and global, space-based (SCIAMACHY and OMI) observations. Journal of Geophysical Research-Atmospheres, 116, Artn D06304, https://doi.org/10.1029/2010jd014758

Lenschow, D.H. (1986) Aircraft Measurements in the Boundary Layer. In: Lenschow D.H. (eds) Probing the Atmospheric Boundary Layer. American Meteorological Society, Boston, MA, https://doi.org/10.1007/978-1-944970-14-7_5

National Institute of Environmental Research (NIER), National Aeronautics and Space Administration (NASA) (2017) KORUS-AQ Rapid Science Synthesis Report, https://espo.nasa.gov/sites/default/files/documents/KORUS-AQ%20RSSR.pdf

Ohara, T., Akimoto, H., Kurokawa, J., Horii, N., Yamaji, K., Yan, X., Hayasaka, T. (2007) An Asian emission inventory of anthropogenic emission sources for the period 1980–2020. Atmospheric Chemistry and Physics, 7, 4419–4444

Qu, Z., Henze, D.K., Li, C., Theys, N., Wang, Y., Wang, J., Wang, W., Han, J., Shim, C., Dickerson, R.R., Ren, X.R. (2019) SO_2 Emission Estimates Using OMI SO_2 Retrievals for 2005-2017. Journal of Geophysical Research-Atmospheres, 124, 8336-8359, https://doi.org/10.1029/2019jd030243

Weil, J.C., Brower, R.P. (1984) An Updated Gaussian Plume Model for Tall Stacks. Journal of the Air Pollution Control Association, 34, 818–827, https://doi.org/10.1080/00022470.1984.10465816